

Evaluation of the performance of a particle concentrator for on-line instrumentation

Saarikoski, S.^{1,2,3}, Carbone, S.¹, Cubison, M. J.^{2,3,*}, Hillamo, R.¹, Keronen, P.⁵, Sioutas, C.⁴, Worsnop, D. R.^{1,5,6} and Jimenez, J. L.^{2,3}

¹Atmospheric Composition Research, Finnish Meteorological Institute, 00101, Helsinki, Finland

²Cooperative Institute for Research in the Environmental Sciences, 80309, Boulder, USA

³Department of Chemistry and Biochemistry, University of Colorado at Boulder, 80309, Boulder, USA

⁴Dept. of Civil and Environmental Engineering, University of Southern California, Los Angeles, CA, 90089, USA

⁵Department of Physics, University of Helsinki, University of Helsinki, FI-00014, Helsinki, Finland

⁶Aerodyne Research Inc., Billerica, MA 01821, USA

*now at Tofwerk AG

Supplements

Table S1. The shift of particles size for monodisperse AS and DOS particles in the m-VACES.

Particle size (nm)	AS % (nm)	DOS % (nm)
50	20 (10)	30 (5.9)
70	7.7 (5.4)	7.7 (5.4)
100	4.0 (4.0)	4.0 (4.0)
200	3.5 (7.0)	3.5 (7.0)
300	0.0 (0.0)	0.0 (0.0)

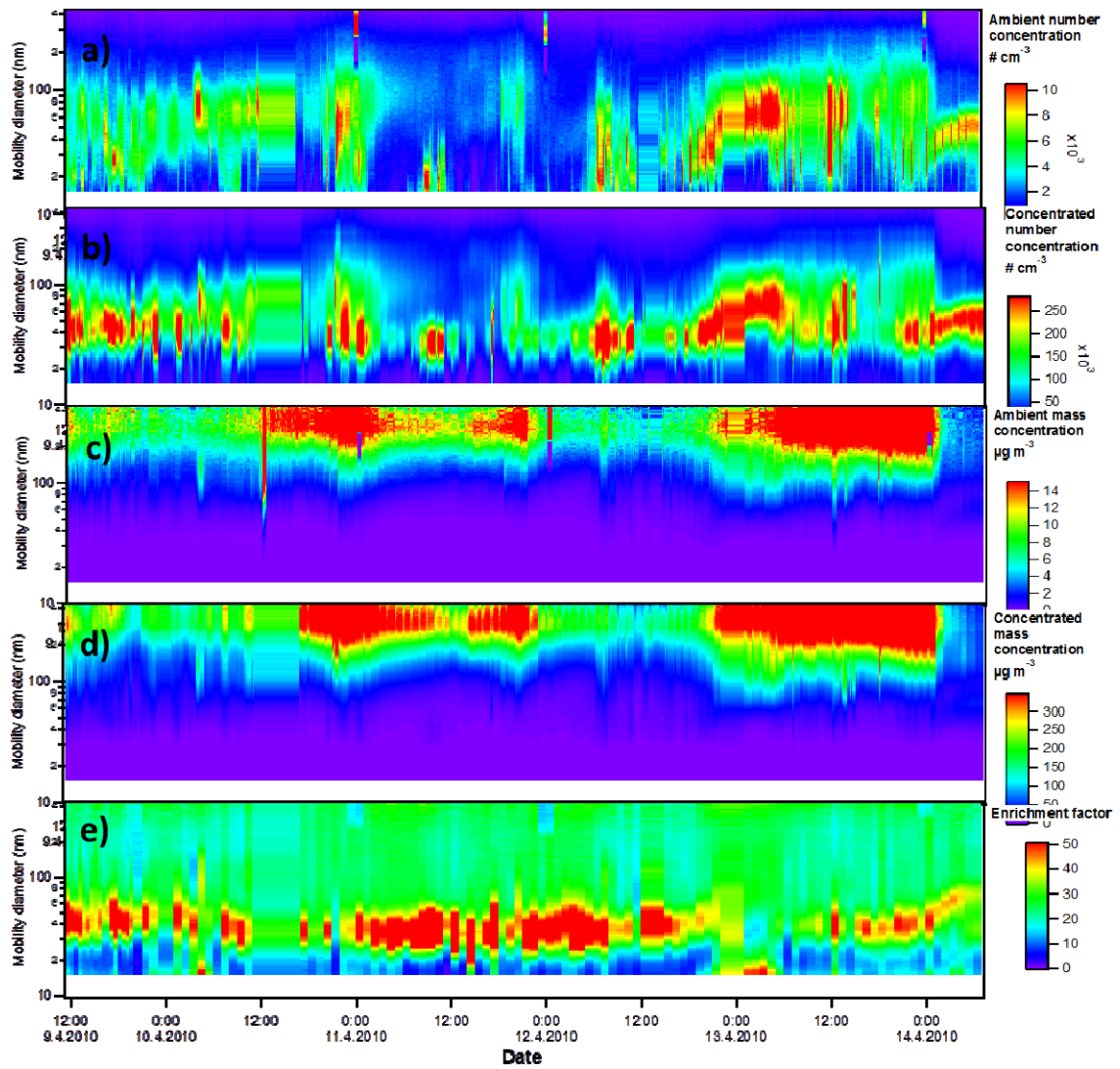


Fig. S1. Time series for the size distributions of particle number (a-b), mass (c-d) and enrichment factor. (a) and (c) are for ambient and (b) and (d) for concentrated aerosol. Particle mass was calculated by using the density of 1.48 g cm^{-3} .

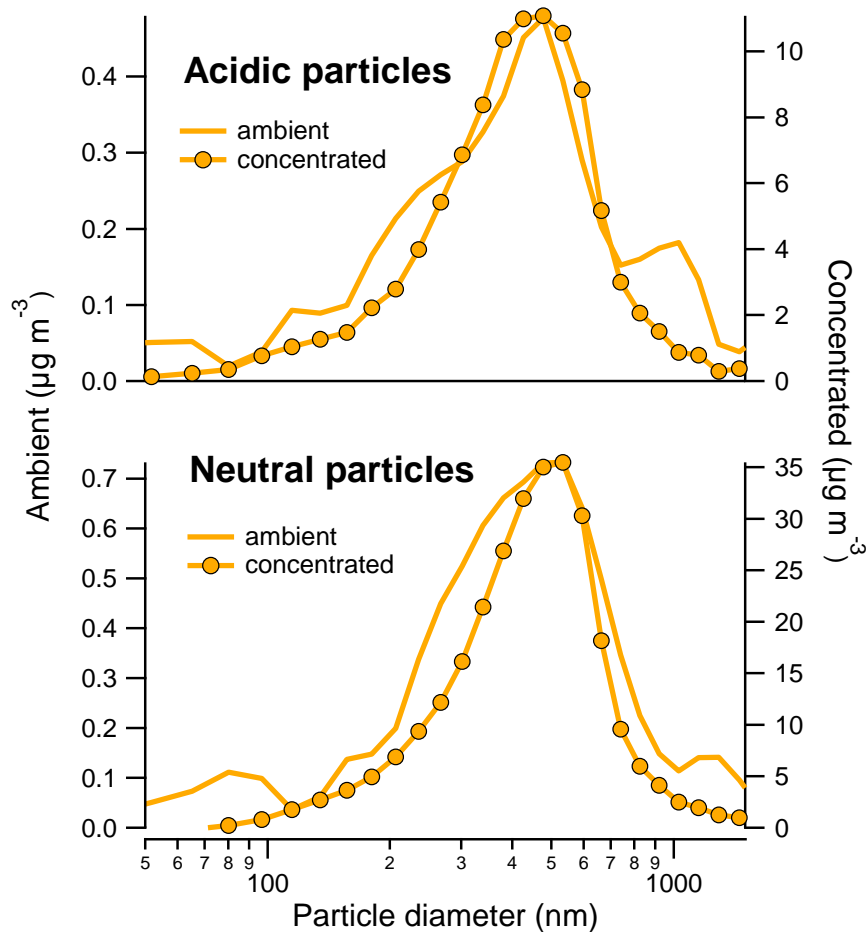


Fig. S2. Size distribution of ammonium during the period when the particles were acidic (April 12, 2010) and nearly neutral (April 13, 2010; 6 am to midnight). Ambient size distributions were smoothed by one point.

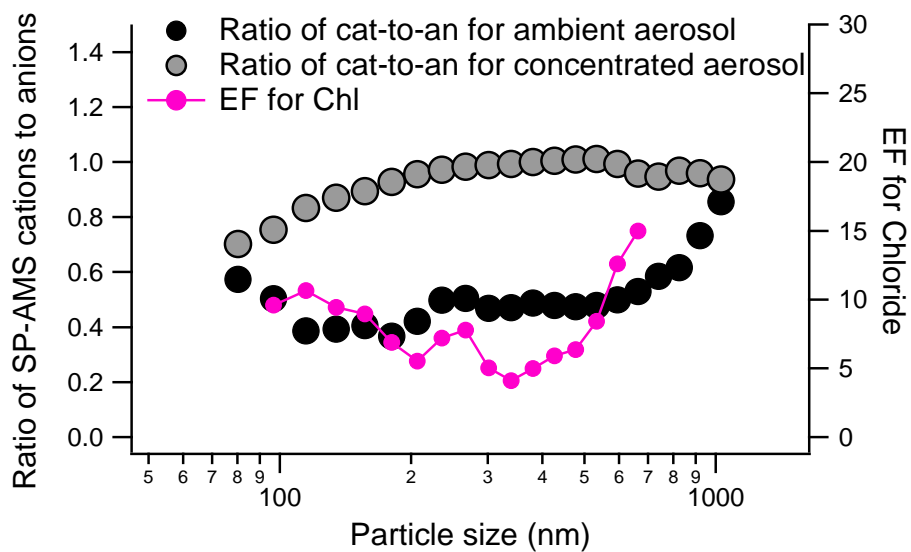


Fig. S3. Ratio of SP-AMS cations to anions for ambient and concentrated particles and EF for chloride as a function of particle size. Average for the whole measurement period. Ratios have been smoothed by 1 point.

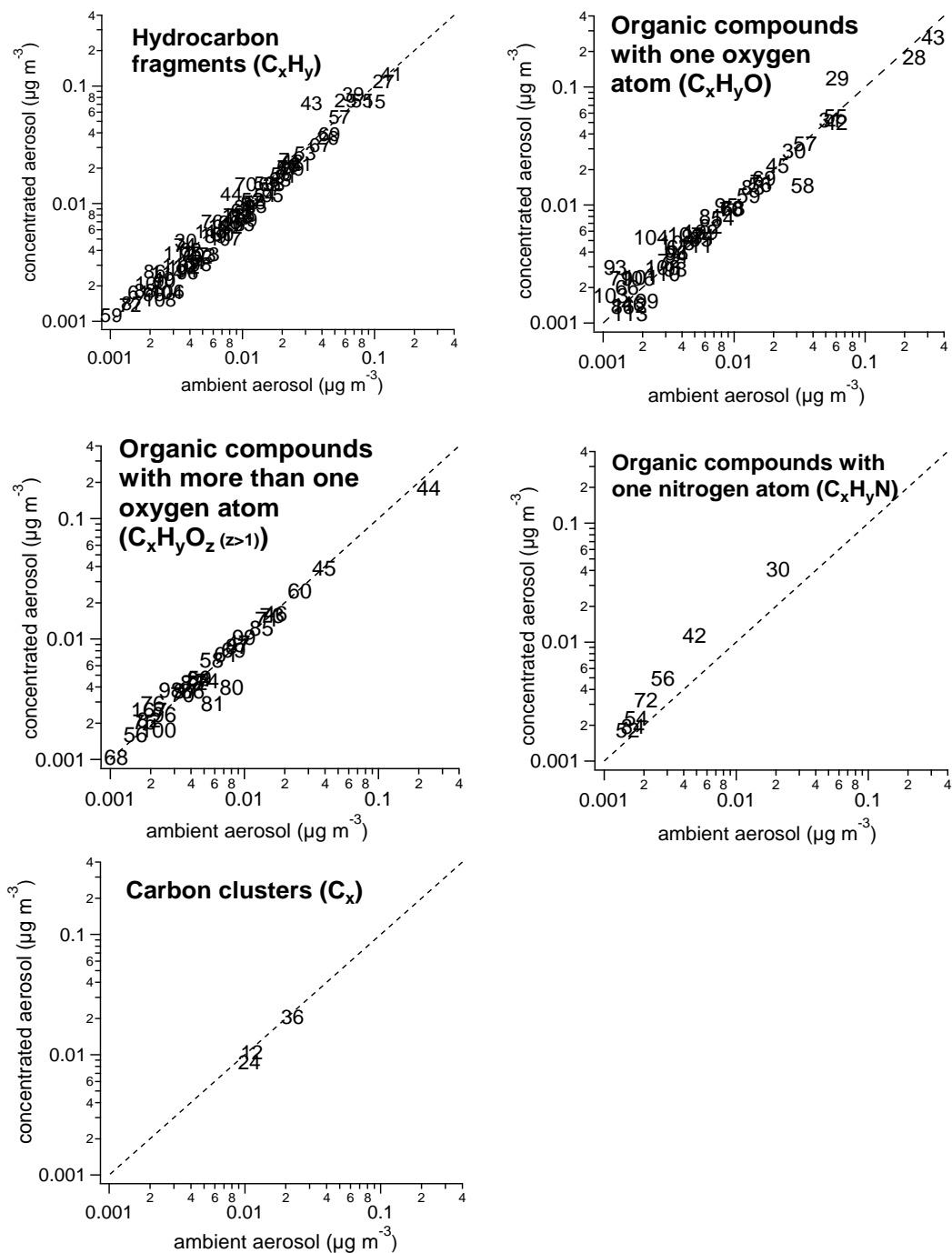


Fig. S4. Scatter plots of the mass fragments in ambient and concentrated OA separated into different compound classes. Carbon clusters (C_x) were measured only with the laser on and the concentration of C_1 (m/z 12) according to the fragmentation Table in Onasch et al. (2012). Concentrated aerosol is divided by the average EF for organics (27.08; a, c-e) and r-BC (37.61; b) (Table 2). One to one ratio is shown by dash lines.

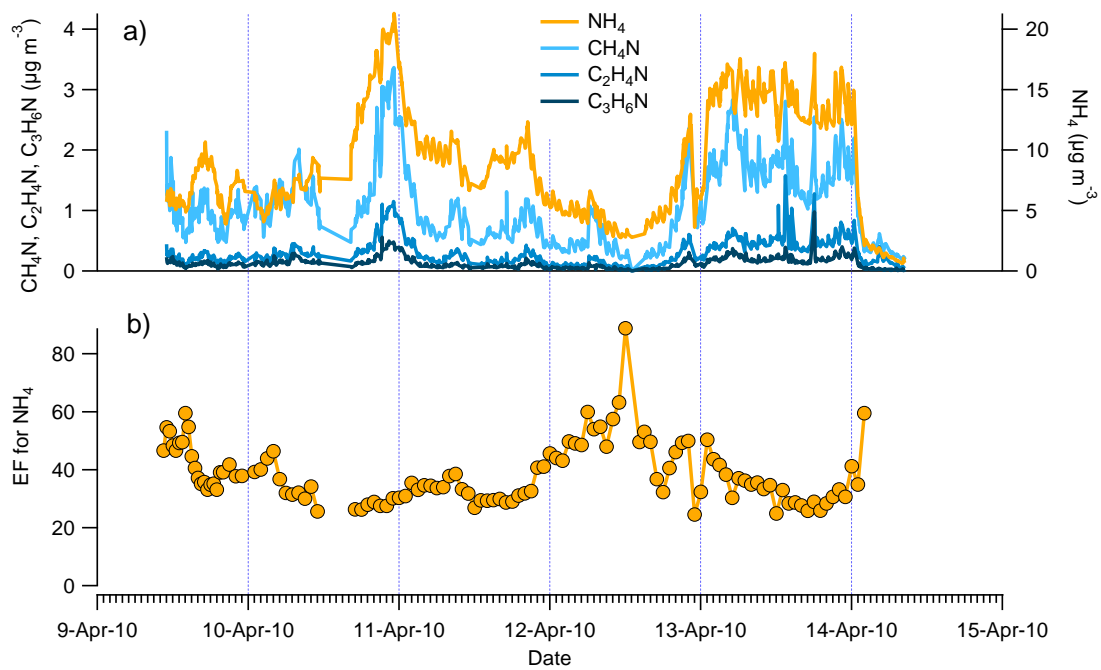


Fig. S5. Time series of ammonium and amines for the concentrated aerosol (a) and the enrichment factor for ammonium (b).

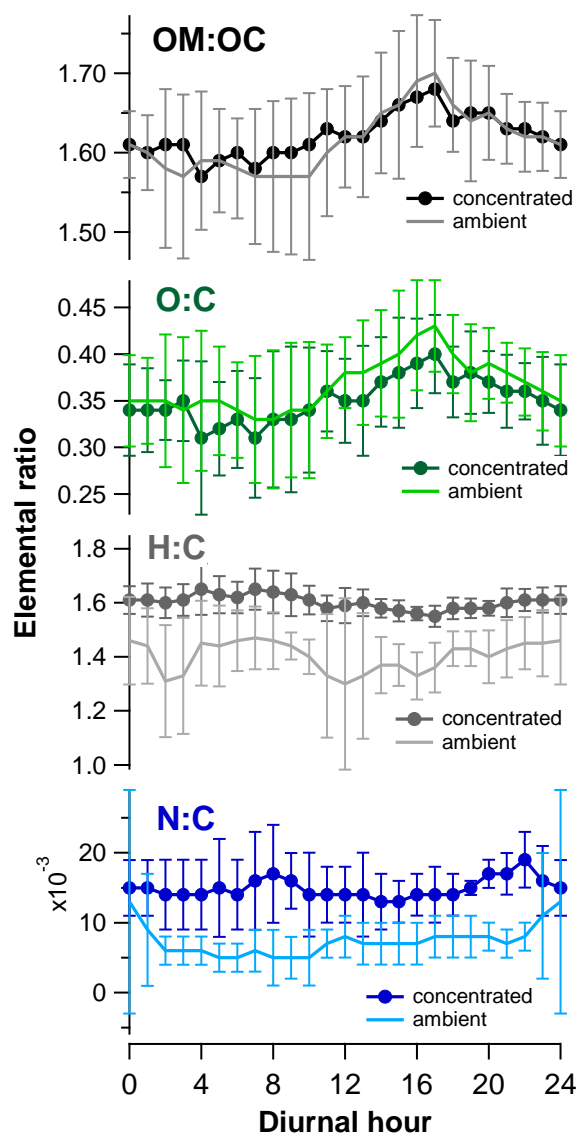


Fig. S6. Diurnal trends for OM:OC, O:C, H:C and N:C for concentrated and ambient OA.

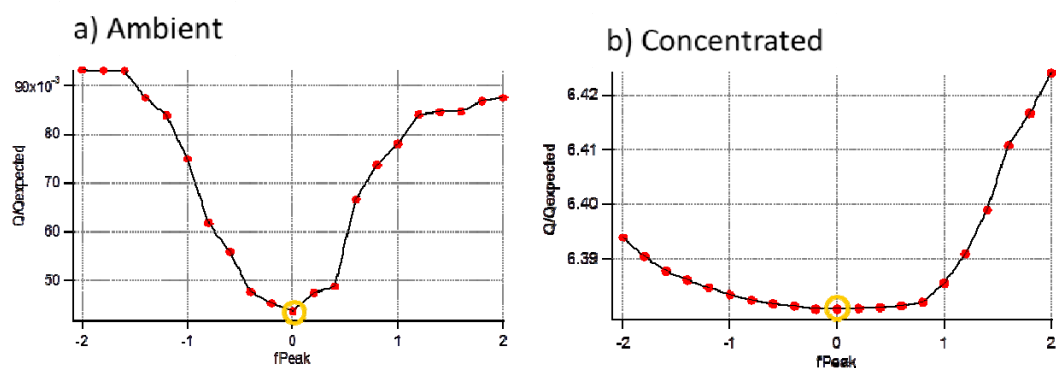
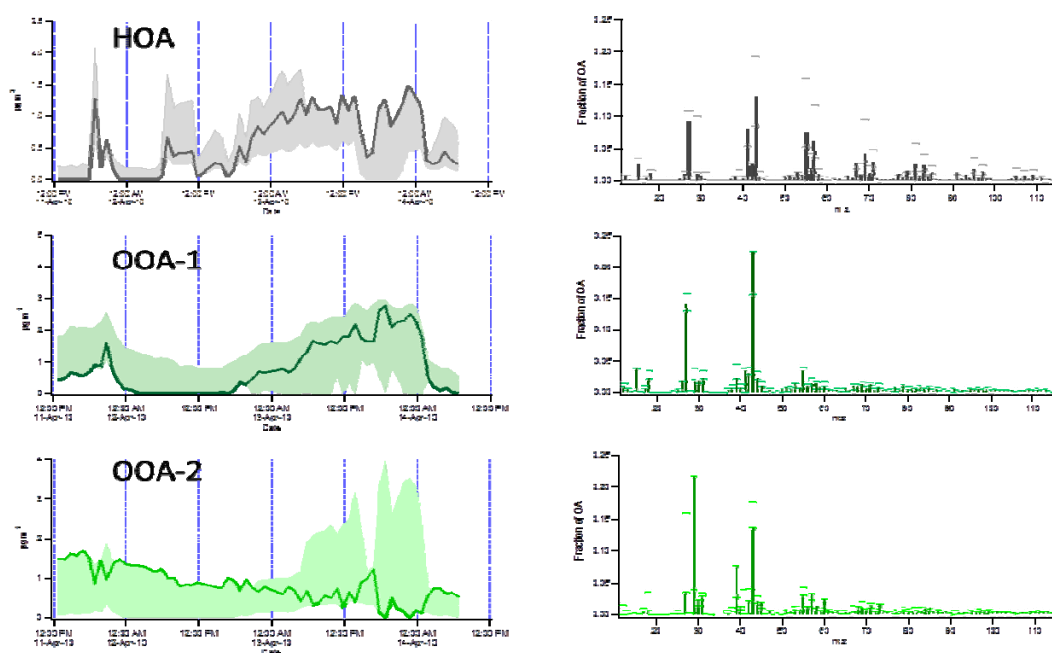


Fig. S8. The variation of Q/Q_{expected} with the value of f_{PEAK} for ambient (a) and concentrated (b) PMF solution.

a) Ambient



b) Concentrated

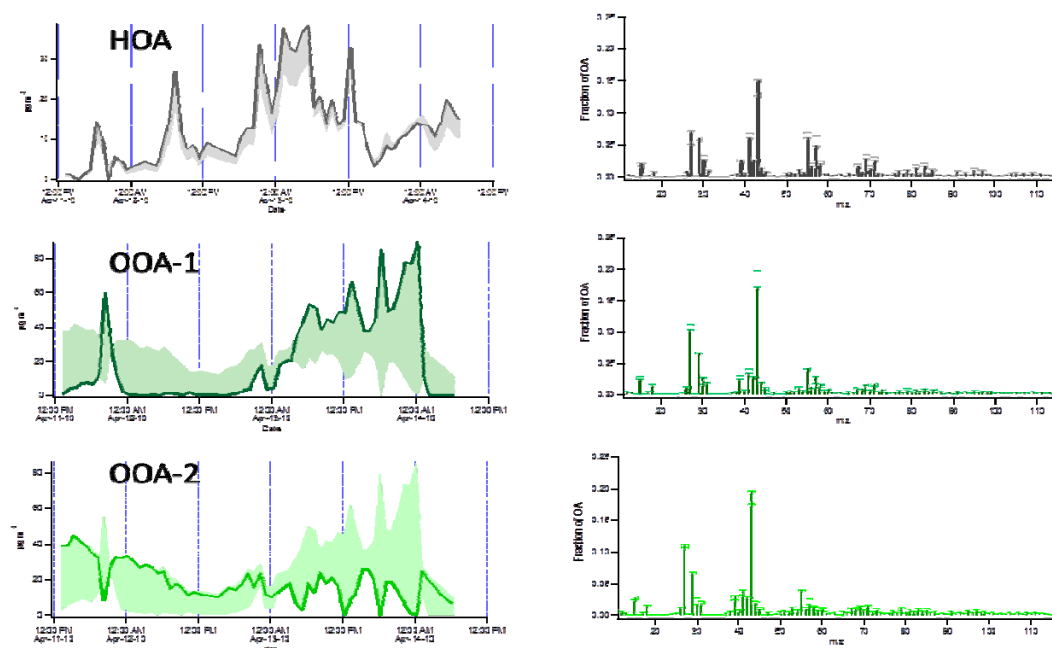


Fig. S9. The variation of time series and mass spectra for the PMF factors with the fPEAK values from -0.4 to 1.6. Ambient (a) and concentrated (b) OA.

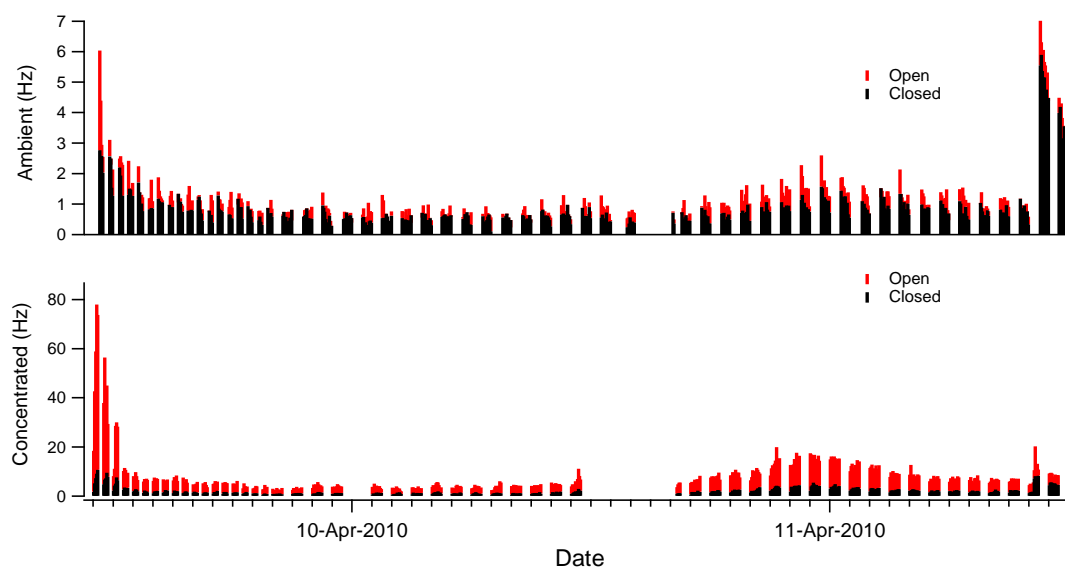


Fig. S10. Slow evaporation of zinc. Open and closed signal for ambient and concentrated aerosol.

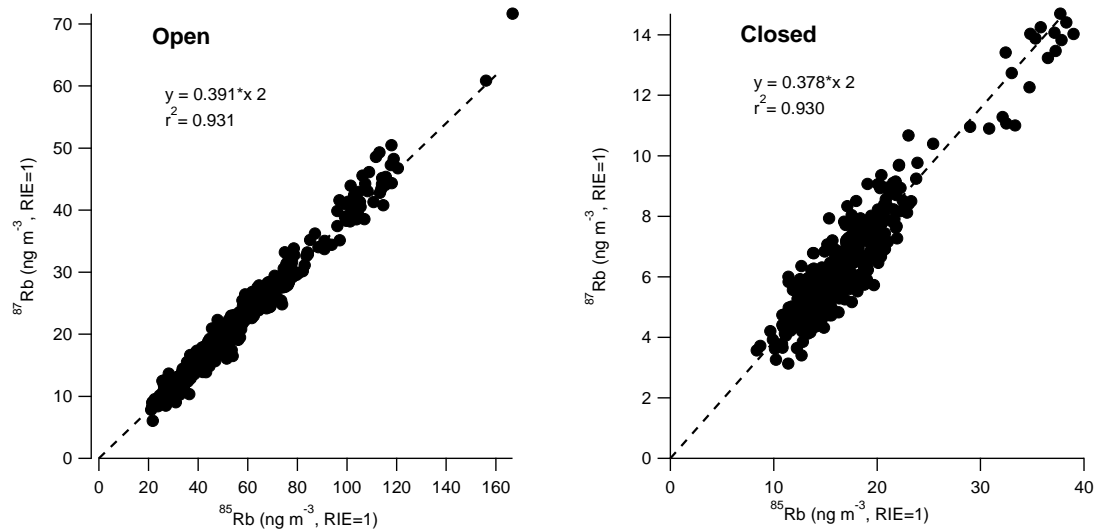


Fig. S11. Scatterplot of signal from ^{87}Rb and ^{85}Rb for open and closed modes. Expected natural isotopic ratio is shown by a dash line.

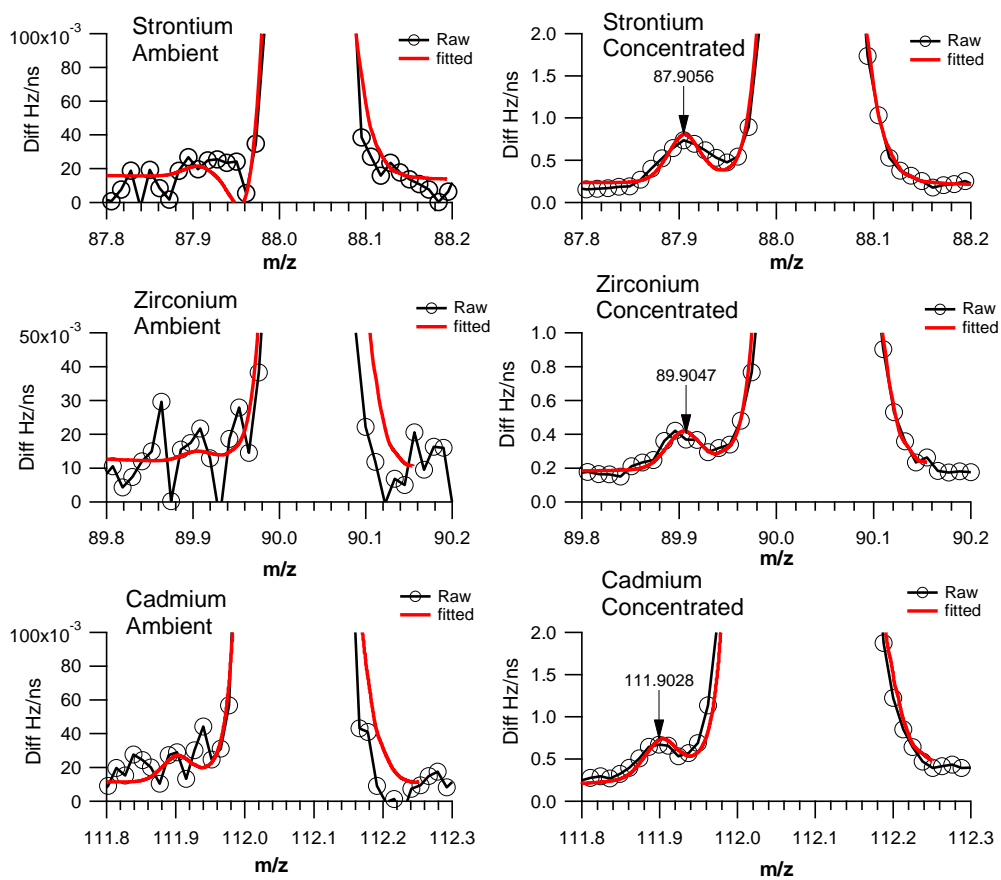


Fig. S12. Strontium, zirconium and cadmium peaks for ambient and concentrated aerosol. Additional isotopes of these ions could not be detected.